

# PARTICLE AND POWER FLUXES DURING AN ELM OBSERVED BY PROBES IN THE DIVERTORS OF ASDEX UPGRADE AND JET

Michael Laux<sup>1</sup>, Stefan Jachmich<sup>2</sup>, Albrecht Herrmann<sup>1</sup>,  
Guy Matthews<sup>3</sup>, Wojciech Fundamenski<sup>3</sup> and  
contributors to the EFDA-JET workprogramme

<sup>1</sup>Max-Planck-Institut für Plasmaphysik, Association EURATOM, Germany

<sup>2</sup>Laboratory for Plasma Physics, Ecole Royale Militaire/Koninklijke Militaire School,  
Association EURATOM-Belgian State, Brussels, Belgium

<sup>3</sup>UKAEA Fusion, Culham Science Center, Abingdon, UK

## Introduction

Arrays of Langmuir probes are integrated into the target plates of the divertors of JET and ASDEX Upgrade to monitor the spatial distribution and temporal evolution of the saturation current  $I_{sat}$ , electron temperature  $T_e$ , and the floating potential  $V_{float}$  [1,2]. Furthermore, particle and power fluxes as well as electron pressure and plasma potential can be inferred from the directly measured parameters using simple model assumptions. As the probes are arranged in an array, profiles and spatial gradients of parameters can also be estimated.

At higher heating powers divertor tokamaks operate in the high-confinement mode (H-mode). Modes localised in the edge region (ELMs) periodically appear in H-mode plasmas in the form of short transient pulses of particles and energy passing the separatrix into the scrape-off layer (SOL) and are transported into the divertor [3,4]. Electrical probes react especially sensitive to these events because ELMs are accompanied by electric fields and currents in SOL and divertor [5,6]. But it can be expected that a diagnostic influenced by a specific disturbance is generally able to provide information on the physical nature of this disturbance.

## Extraction of coherently averaged ELM signals

ELM series show repetitive as well as stochastic aspects. To separate both a special technique was developed that evaluates a coherently averaged ELM together with the evolution of certain ELM characteristics for a given ELM-series. The averaging procedure generally relies on the existence of a measured parameter (the so-called marker) that can be used as ELM indicator in the sense that an easily recognizable feature of it (like e.g. the peaking) is believed to be rigidly related to a distinct moment of time during any individual ELM. In the examples reported below the peaking of the  $D_\alpha$  intensity was used as the marker to determine ELM moments and intervals in the time-series of any parameter measured during the same ELM phase. These intervals then contain just one ELM and one time tick marking the selected moment during that ELM (like e.g. the maximum). Afterwards all intervals of the considered signal can be overlayed with respect to the marker tick and averaged to produce a coherently averaged ELM signal. In the examples below the overall number of marker-signal datapoints above a given signal-level as a function of that level was constructed and a location on the slope is selected as cut level for the whole time series (in analogy to the method of pulse height analysis in nuclear physics). The choice is slightly arbitrary (depending on the kind

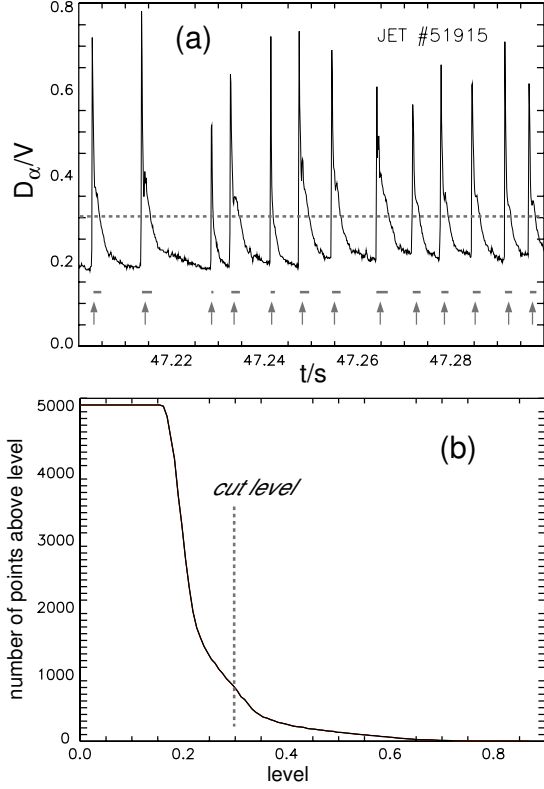


Figure 1: (a)  $D_\alpha$  ELM series (ELM intervals and maxima indicated), (b) number of values above level (selected cut level indicated)

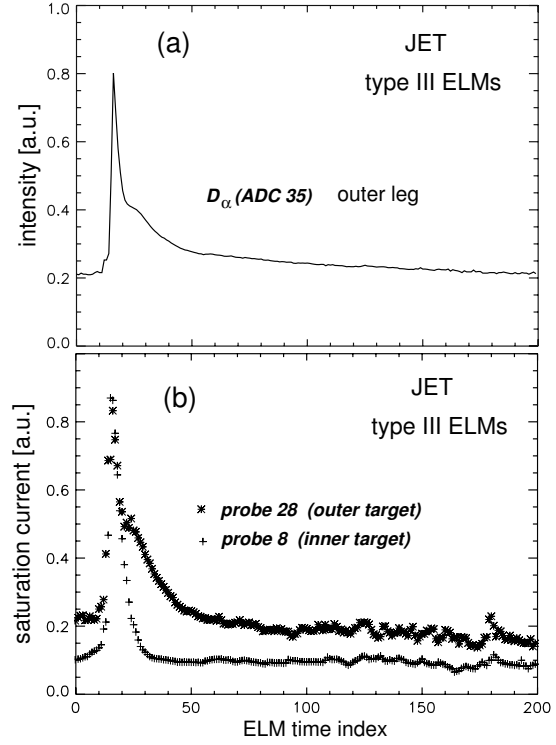


Figure 2: (a) coherently averaged  $D_\alpha$  ELM, (b) coherently averaged  $I_{sat}$  ELMs for the inner and outer leg

of ELMs one want to accept) but can be checked using the standard deviations for the ELM series described below. The method needs no prior knowledge as e.g. a preliminary estimate of the ELM frequency. In essence coherent averaging reduces the noise by smearing ELM to ELM changes out and extract the typical behavior for the whole ELM series. In addition few principal moments (the integral over the signal, the maximum value and its location) are calculated for every individual ELM. Using the average ELM the standard deviation of individual ELMs can be estimated with respect to the average as a figure of merit to identify outliers or recognize different kinds of ELMs in the series. Of course the ELM identification part of the method can also be applied to unravel the disturbing interference of ELMs in all kinds of slow variations (like slow motions of the strike zone position or slow ramps of the probe voltage).

### Examples of coherently averaged ELM signals

Examples of coherently averaged ELM signals for JET and AUGD H-modes are presented below, whereas the accompanying evolutions of ELM moments are reported in [7]. Fig.1 shows the  $D_\alpha$  intensity for the outer divertor leg of JET (a) together with the functional dependence of the number of points exceeding a given level for that time series (b). The different signal levels within an ELM and in between ELMs allow the determination of a cut level defining the intervals of individual ELMs. The maximum  $D_\alpha$ -signal in every interval then determines the tick. On the basis of the field of these marker ticks

$I_{sat}$  and  $D_\alpha$  every time series observed during the same ELMy periode can now be coherently averaged. The averaged  $D_\alpha$  ELM from the marker signal itself is shown in fig.2 demonstrating the remarkable noise reduction.

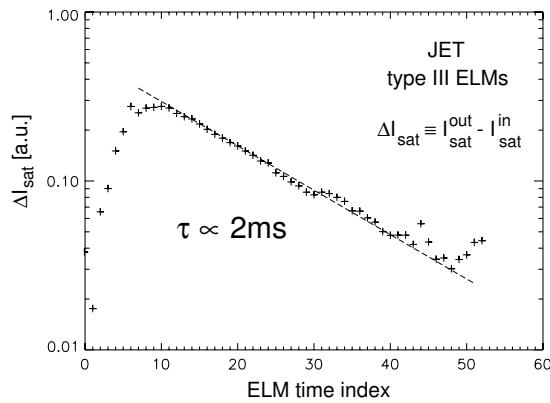


Figure 3: exponentially decaying second component at the outer leg

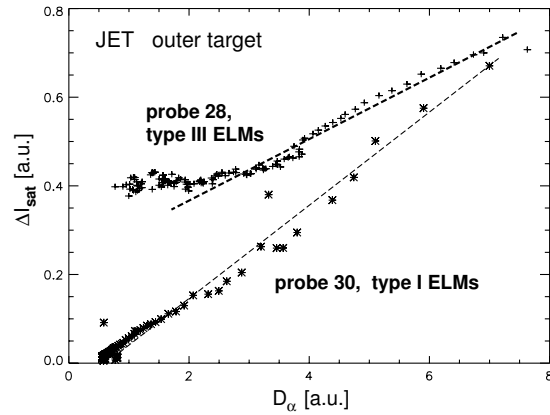


Figure 4: coherently averaged  $I_{sat}$  versus  $D_\alpha$  for both ELM types

A comparison of the averaged  $I_{sat}$  signals observed by probes situated in the SOL just outside separatrix in the inner and outer legs of JET allows to postulate a second component to the outer leg in a type III ELM-series (fig.3). This component behaves clearly exponential in time ( $\tau \approx 2ms$ ). For type I ELMs an additional component to the inner leg was observed. The comparison of the averaged  $D_\alpha$  with the averaged  $I_{sat}$  shows an almost linear relation throughout the whole ELM event (fig.4). For the divertor of ASDEX Upgrade the influence of an ELM has partly a different character. In the early phase of an AUGD type I ELM a short highly turbulent period exists that is well pronounced in  $D_\alpha$  and  $I_{sat}$  even after averaging over more than 1000 individual ELMs (fig.5). Outside that periode the averaged ELM signals are very smooth and free of noise. Most remarkable is the fact that the ion saturation current does change sign during the turbulent periode, thereby loosing its original physical meaning. At JET no such turbulent behaviour is observed, but averaging  $T_e$  or  $V_{float}$  reveals that both peak clearly during the rise of the accompanying  $I_{sat}$  and show large excursions (fig.6).

Because of the structure of the  $T_e$  evolution and its shift with respect to  $I_{sat}$  the temporal evolution of the power to the plate (using a conservative sheath transmission factor) can also be very complex. Sometimes such multiple peaking power densities have been observed by thermography. Assuming a simple model for the sheath the plasma potential during the type III ELM in JET was calculated and found to be unexpectedly simple (fig.7). As a next step plasma potentials have been constructed for neighbouring target probes in the outer leg of the JET divertor giving the typical evolution of the radial electric field (fig.8).

## Conclusions

The coherent averaging methode is able to deliver the temporal evolution of plasma parameters during an ELM showing remarkably low noise. The averaged  $I_{sat}$  and  $D_\alpha$  are usually linearly related during the ELM. As a consequence of the noise reduction distinct components to  $I_{sat}$  and  $D_\alpha$  could be identified. Additionally, reliable curves for the temporal evolution of plasma potential, power flux to the target, and the radial

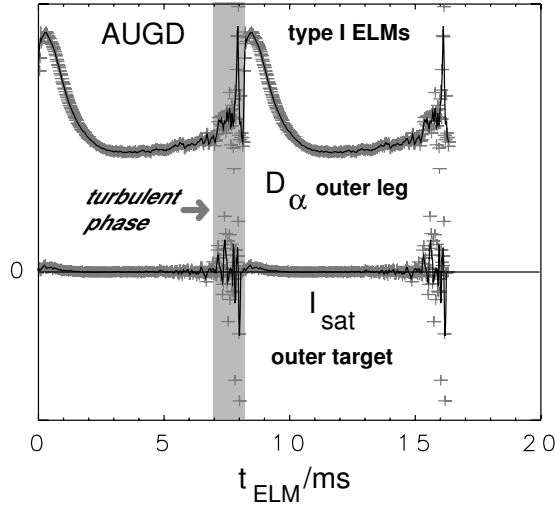


Figure 5: coherently averaged  $D_\alpha$  and  $I_{sat}$  from AUGD showing the early turbulent phase

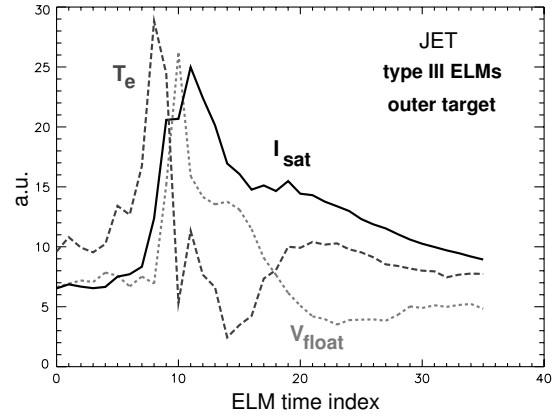


Figure 6: coherently averaged  $T_e$ ,  $V_{float}$  peaking earlier than  $I_{sat}$  during a JET ELM

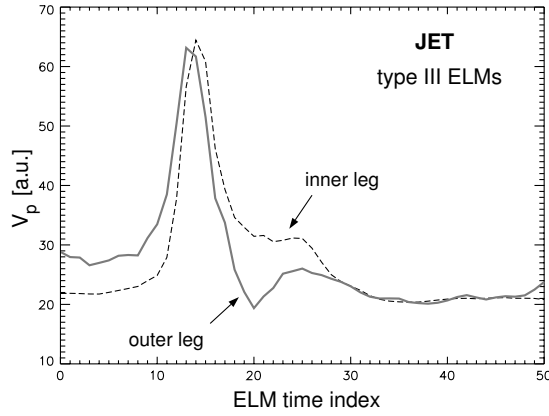


Figure 7: Plasma potential calculated from coherently averaged  $T_e$  and  $V_{float}$  for a JET ELM

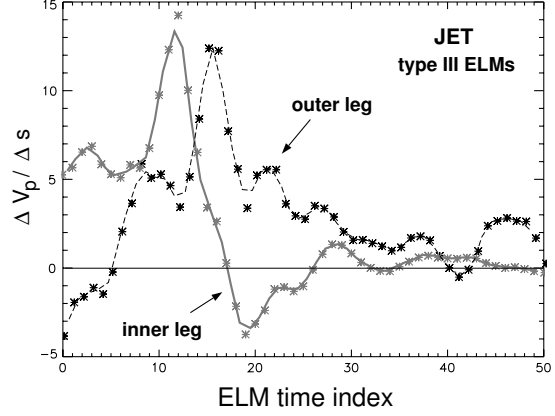


Figure 8: estimated electric field ( $\Delta V_p/\Delta s$ ) along the outer JET target close to the separatrix

electric field have been derived for JET. A turbulent phase was identified during the ELM rise (more pronounced at AUGD than at JET) seriously challenging the probe interpretation.

## References

- [1] G.F. Matthews, S.D. Davies, R.D. Monk, Contrib. Plasma Phys. 36 (1996) S, 29-36
- [2] M. Weinlich, A. Carlson, Contrib. Plasma Phys. 36 (1996) S, 53-60
- [3] H. Zohm, Plasma Phys. Contr. Fusion 38(1996),105-128
- [4] W. Suttrop, Plasma Phys. Contr. Fusion 42 (2000), A1-A14
- [5] J. Lingertat, M. Laux, R.D. Monk, J. Nucl. Mater. 290-293 (2001), 896-899
- [6] J. Lingertat, K. Günther, A. Loarte, J. Nucl. Mater. 220/222 (1995), 198-202
- [7] S. Jachmich et.al., "Novel methode to study SOL-response to ELMs by divertor target probes in JET" this conference